

# RSC Advances



This is an *Accepted Manuscript*, which has been through the Royal Society of Chemistry peer review process and has been accepted for publication.

*Accepted Manuscripts* are published online shortly after acceptance, before technical editing, formatting and proof reading. Using this free service, authors can make their results available to the community, in citable form, before we publish the edited article. This *Accepted Manuscript* will be replaced by the edited, formatted and paginated article as soon as this is available.

You can find more information about *Accepted Manuscripts* in the [Information for Authors](#).

Please note that technical editing may introduce minor changes to the text and/or graphics, which may alter content. The journal's standard [Terms & Conditions](#) and the [Ethical guidelines](#) still apply. In no event shall the Royal Society of Chemistry be held responsible for any errors or omissions in this *Accepted Manuscript* or any consequences arising from the use of any information it contains.

Cite this: DOI: 10.1039/c0xx00000x

www.rsc.org/xxxxxx

ARTICLE TYPE

# The temperature-dependence of the structure-directing effect of 2-methylpiperazine in the synthesis of open-framework aluminophosphates

Pai Huang<sup>a‡</sup>, Jun Xu<sup>b‡</sup>, Chao Wang<sup>b</sup>, Feng Deng<sup>b</sup> and Wenfu Yan<sup>a\*</sup>

Received (in XXX, XXX) XthXXXXXXXXXX 20XX, Accepted Xth XXXXXXXXXXXX 20XX  
DOI: 10.1039/b000000x

Heating the same initial mixture with the composition of Al<sub>2</sub>O<sub>3</sub>:P<sub>2</sub>O<sub>5</sub>:1.5 2-methylpiperazine:125 H<sub>2</sub>O at 150 and 200°C, respectively, two layered aluminophosphates were obtained. The crystallization processes of these layered aluminophosphates were investigated using multiple techniques. The change in the pH values of the solutions, the change in the concentrations of Al and P in the liquid phases, and the evolution of the coordination states of Al and P in the solid products were monitored. The “reverse temporal evolution” analyses of each structure showed that the core units or the possible onsets (nuclei) of crystallization of each structure were significantly different from each other. The results showed that the heating temperature altered the structure-directing effect of 2-methylpiperazine and the crystallization process of the initial mixture via changing the structure and chemical properties of the structure-directing agent of 2-methylpiperazine, the equilibrium of the reactions occurring among the source materials, and the assembly of the inorganic oligomers.

## 1. Introduction

Zeolites and the related open-framework crystalline materials have attracted great interest due to their extensive applications in catalysis, ion-exchange, separation, and adsorption techniques.<sup>1-4</sup> The synthesis of these crystalline materials typically involved mixing the sources of the inorganic ions, the solvent, and, generally, an organic species, which is usually called the “template” or the “structure-directing agent”, and heating the resulting mixture in an autoclave at an elevated temperature for a period ranging from a few hours to weeks. The introduction of the organic species into the synthetic system and the extension of the material’s composition from aluminosilicate to aluminophosphate significantly increased the structural diversity of the microporous crystalline materials and the related open-framework materials.<sup>5-11</sup> However, the type of structure that can be crystallized from a batch synthesis is controlled by many synthetic parameters. Among the synthetic parameters, the most important is the “template” or the “structure-directing agent”. Certain structures will not form in the absence of a specific organic additive. The structure-directing effect, especially in the synthesis of the microporous or open-framework aluminophosphates, is explained by the steric and electronic influences of these organic additives.<sup>1, 12, 13</sup> The structure-directing effect of the organic species is due to its charge distribution, size and geometric shape. However, the exact role of the structure-directing agents is not understood. In addition, it has been experimentally observed that one template can direct many structures and one structure can be directed by many templates,

which suggests that the structure-directing effect of a template is affected by many other factors. These factors are part of the structure-directing effect of a template. Thus, the investigation of the influence of other factors on the structure-directing effect of a template is very important in correctly understanding the nature of structure-directing effect in the crystallization of microporous materials.

The difficulty in investigating the structure-directing role of the organic additives arises from the complexity of the hydro/solvothermal crystallizations and the lack of structural information about the species that are formed during the different synthesis stages.<sup>4</sup> Therefore, enhanced efforts and new ideas are needed for a better understanding of the role of the organic additives in the synthesis of microporous crystalline materials.<sup>14-51</sup> To investigate the influence of other factors on the structure-directing effect of a template, we need to keep all other synthetic parameters constant and change only one factor in the synthesis.

In this study, we investigated the crystallization processes of two layered aluminophosphates that were synthesized from the same initial mixture with the optimized molar composition, in which 2-methylpiperazine (denoted MeP) was used as the structure-directing agent.<sup>52</sup> The heating temperatures for these two layered aluminophosphates were 150 and 200°C; thus, these two compounds were named APMep150 and APMep200, respectively. To obtain the pure phase of these two compounds, the composition of the initial mixture was optimized from that for previous study<sup>52</sup> to Al<sub>2</sub>O<sub>3</sub>:P<sub>2</sub>O<sub>5</sub>:1.5MeP:125 H<sub>2</sub>O. We investigated the influence of the heating temperature on the crystallization process of these two layered aluminophosphates, on the structure-directing effect of 2-methylpiperazine, and on

the core units or the possible onsets (nuclei) of crystallization for both compounds.

## 2. Experimental section

### 2.1 Synthesis

The aluminium and phosphorus sources used were boehmite (Catapal B, 72.7%  $\text{Al}_2\text{O}_3$ , Sasol) and phosphoric acid (85 wt%  $\text{H}_3\text{PO}_4$ ), respectively. The structure-directing agent was 2-methylpiperazine ( $\text{C}_5\text{H}_{12}\text{N}_2$ , MeP). The procedure used for the preparation of the reaction mixture was as follows: 4.6 g of 85wt% phosphoric acid was stirred with 45mL of water, and 2.8 g of boehmite was added to the mixture. After the mixture was thoroughly stirred for 1 h, 3.0 g of 2-methylpiperazine was added with continuous stirring. The gel continued to be stirred for 1 h at an ambient temperature to ensure homogeneity. The same amount of the reaction mixture with a molar ratio of  $\text{Al}_2\text{O}_3:\text{P}_2\text{O}_5:1.5\text{MeP}:125\text{H}_2\text{O}$  was loaded into several Teflon-lined autoclaves using a syringe while stirring. The autoclaves were then placed in a pre-heated oven at 150°C (for APMep150) or 200 °C (for APMep200). The autoclaves were quickly loaded into the oven, and the timed heating began. The autoclaves were heated for different periods of time and quenched in cold water. The pH of the liquid phase was measured. The liquid and solid phases of the product were separated by centrifugation (9500 rpm or 8475 g), and the solid phase was freeze-dried without further washing with water. The dried samples were sealed for subsequent characterization. The concentration of Al and P in the liquid phase was measured.

### 2.2 Characterization

The NMR experiments were performed on a Varian Infinity-plus 400 spectrometer operating at a magnetic field strength of 9.4 T. The resonance frequencies at this field strength were 161.9 and 104.2 MHz for  $^{31}\text{P}$  and  $^{27}\text{Al}$ , respectively. A Chemagnetics 5 mm triple-resonance MAS probe with a spinning rate of 8 kHz was employed to acquire the  $^{31}\text{P}$  and  $^{27}\text{Al}$  NMR spectra. The  $^{27}\text{Al}$  MAS spectra were acquired using a single pulse sequence with a short radio frequency (rf) pulse of 0.5 s (corresponding to a  $\pi/15$  flip angle) and a pulse delay of 1.0 s. The pulse length for  $^{27}\text{Al}$  was measured using a 1 M  $\text{Al}(\text{NO}_3)_3$  solution. The single-pulse  $^{31}\text{P}$  MAS NMR experiments with  $^1\text{H}$  decoupling were performed with a 90° pulse width of 4.6  $\mu\text{s}$ , a 180 s recycle delay, and a  $^1\text{H}$  decoupling strength of 42 kHz. The chemical shifts were referenced to an 85%  $\text{H}_3\text{PO}_4$  solution for  $^{31}\text{P}$  and a 1 M  $\text{Al}(\text{NO}_3)_3$  solution for  $^{27}\text{Al}$ .

The powder X-ray diffraction (XRD) patterns were recorded on a Rigaku diffractometer that was equipped with a graphite monochromator using Cu K $\alpha$  radiation ( $\lambda=1.5418\text{ \AA}$ ). The pH values of the liquid phases were measured with a Sartorius PB-10 pH meter. The inductively coupled plasma atomic emission spectroscopy (ICP-AES) analysis was performed on a Perkin-Elmer Optima 3300DV spectrometer. Scanning electron microscopy (SEM) images were obtained on a JEOL JSM6510 instrument with an acceleration voltage of 20 kV.

## 3. Results and discussion

According to Tuel et al.,<sup>52</sup> the empirical formula of APMep150 is

$[\text{Al}_6\text{P}_8\text{O}_{32}(\text{H}_2\text{O})_2]\cdot[\text{C}_5\text{N}_2\text{H}_{14}]_3\cdot 10\text{H}_2\text{O}$ . The 2-methylpiperazine molecules were found to be doubly protonated and located in the interlayer region. The structure of APMep150 is composed of a two-dimensional macroanionic  $[\text{Al}_3\text{P}_4\text{O}_{16}]^{3-}$  layer, consisting of a network of 4-, 6-, and 12-membered rings (MRs). Except for the tetrahedrally coordinated Al atoms, 1/6 of the Al atoms are octahedrally coordinated to two additional water molecules with distances of 2.250 and 2.323  $\text{\AA}$ , resulting in a formula for the inorganic layer of  $[\text{Al}_5\text{P}_8\text{O}_{30}\cdot\text{AlO}_2(\text{H}_2\text{O})_2]^{3-}$ . The Al atoms are connected to four P tetrahedra, whereas the P tetrahedra are linked to three Al tetrahedra and possess a terminal P=O bond that points toward the interlayer space. The 6-MRs are capped with a P tetrahedron, thus forming the “capped 6-MR” units. There are two and four crystallographically independent Al and P atoms in the unit cell, respectively. The detailed topology of the inorganic layer and the labeling scheme of the atoms are shown in Fig. 1(a).

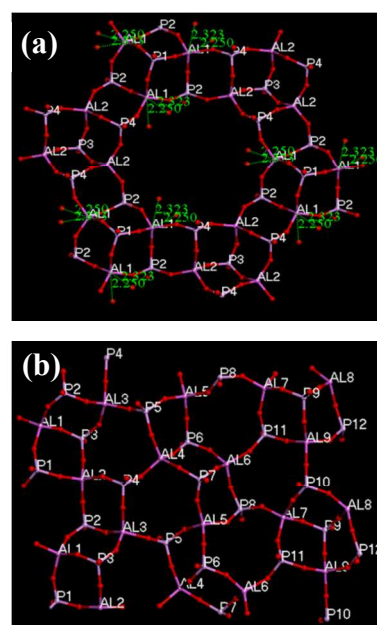


Fig. 1 The inorganic layers of the APMep150 (a) and APMep200 (b).

The empirical formula of APMep200 is  $[\text{Al}_9\text{P}_{12}\text{O}_{48}]\cdot[\text{C}_5\text{N}_2\text{H}_{14}]_{4.5}\cdot 2.5\text{H}_2\text{O}$ ,<sup>52</sup> and the 2-methylpiperazine molecules were found to be doubly protonated and located in the interlayer region. The structure of APMep200 is nearly identical to that of AP2pip, which has an empirical formula of  $[\text{Al}_9\text{P}_{12}\text{O}_{48}]\cdot[\text{C}_4\text{N}_2\text{H}_{12}]_{4.5}\cdot 5\text{H}_2\text{O}$  and is synthesized in the presence of piperazine.<sup>53</sup> The structure of APMep200 is composed of a two-dimensional macroanionic  $[\text{Al}_3\text{P}_4\text{O}_{16}]^{3-}$ , in which both the aluminium and the phosphorus atoms are tetrahedrally coordinated and are strictly alternating. The Al tetrahedra are connected to four P tetrahedra, whereas the P tetrahedra are linked to three Al tetrahedra and possess a terminal P=O bond that points toward the interlayer space. There are nine and twelve crystallographically independent Al and P atoms in the unit cell, respectively. The detailed topology of the inorganic layer and the labeling scheme of the atoms are shown in Fig. 1(b).

### 3.1 X-ray diffraction investigation of the crystallization processes of APMep150 and APMep200

Fig. 2 shows the simulated XRD patterns of APMeP150 (a) and APMeP200 (b) and the experimental patterns of the solid samples, which were isolated throughout the hydrothermal treatment period. The SEM images of the as-synthesized APMeP150 and APMeP200 can be found in Fig.S1 in the Supporting Information. The concentrations of Al and P and the pH values of the liquid phases in the corresponding products are plotted in Fig.S2 and Fig.S3 in the Supporting Information, respectively. The Al and P concentrations and the pH values are provided in Tables S1-S4 in the Supporting Information.

The initial mixture was heated to 150°C, and long-range ordering of APMeP150 was observed after 60 minutes of heating (Fig. 2(a)). The concentration of Al in the liquid phase was low and remained nearly constant during the hydrothermal crystallization process. However, the concentration of P initially increased and then decreased during the subsequent hydrothermal treatment. The concentration of P reached a maximum when long-range ordering began (after 40-60 minutes of heating, Fig. 2(a)). Likewise, the pH of the solution initially decreased and subsequently increased during the hydrothermal treatment period. When the initial mixture was heated to 200°C, no long-range ordering was observed after 30 minutes; however, after 50 minutes of heating, the appearance of long-range ordering of the APMeP200 was observed (Fig. 2(b)). Similarly, the concentration of Al in the liquid phase was low and remained nearly constant during the hydrothermal crystallization process. A slight increase in the concentration of P was observed just before long-range ordering of the APMeP200 (after 30-50 minutes of heating, Fig. 2(b)). Therefore, the pH was expected to increase during the hydrothermal treatment. Fig. 2 shows that highly crystalline and pure APMeP150 and APMeP200 were obtained when the initial mixture was heated for 720 minutes.

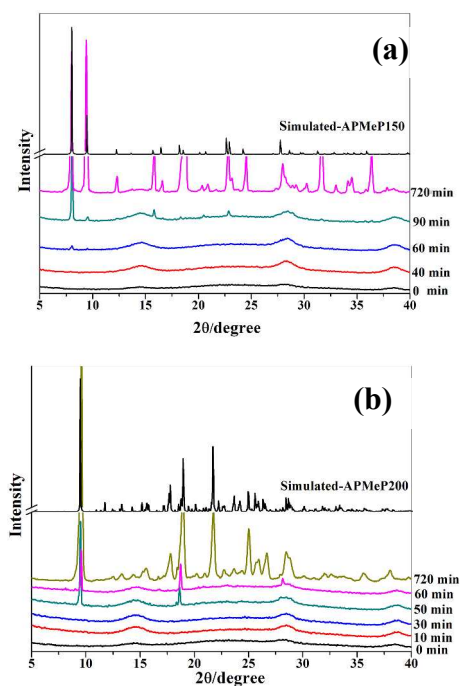


**Fig. 2** The simulated XRD patterns of APMeP150 (a) and APMeP200 (b) and the experimental patterns of the solid samples that were isolated throughout the hydrothermal treatment period.

### 3.2 NMR study of the crystallization process of APMeP150 and APMeP200

The NMR signal is sensitive to the structural changes that result from short-range ordering; this property can be used to detect a change in the local environment of the small building fragments that are involved in crystal formation and growth during the crystallization process. To obtain detailed information about the coordination state of Al and P in the small building fragments that are formed during the crystallization process and their evolution with time, we characterized the products that were isolated throughout the hydrothermal treatment period using a solid state NMR technique. Fig. 3 shows the  $^{27}\text{Al}$  MAS NMR spectra of the isolated solid samples that were obtained throughout the hydrothermal treatment period during APMeP150 (a) and APMeP200 (b) crystallization. In the initial mixture (Fig. 3), the Al source produced a typical signal at 6.9 ppm, and this signal was observed in the majority of the samples throughout the crystallization process, indicating that the Al atoms that were involved in the crystallization process were gradually released from the aluminium source. The existence of a tetrahedral Al was confirmed by the appearance of a resonance at 44.0 ppm, suggesting that either an Al<sub>2</sub>-centered and a portion of an Al<sub>1</sub>-centered pentamer or small fragments of APMeP150 having a large size have been formed (see Fig. 1(a)). A signal at -11.3 ppm, which was attributed to the typical octahedral Al, was also observed, suggesting that six-coordinated Al<sub>1</sub>-centered pentamers or small fragments of a large size of APMeP150 have also been formed (see Fig. 1(a)). When the initial mixture was heated to 150°C, the intensity of the signal at 44.0 ppm initially decreased significantly (after 40 minutes), and then gradually increased (after 60 and 90 minutes), suggesting that these small fragments were first dissolved then reformed when heated to 150°C (Fig. 3(a)). After 720 minutes of heating, the signal at 44.0 ppm shifted to 42.1 ppm and reached a maximum intensity, corresponding to the highly crystalline and pure APMeP150. Interestingly, the signal at 42.1 ppm in present study appears at 38 ppm in the previous study of the synthesis of APMeP150,<sup>52</sup> which also reports the weak signals between -20 and -50 ppm, corresponding to six-coordinated Al. However, these resonances were not observed in the present study. The weak signal that was attributed to a six-coordinated Al (at -11.3 ppm) gradually disappeared during the crystallization process. These results suggest that the crystallization pathway of APMeP150 in this study is different to that in the original literature due to a different composition of the initial mixture even though the structure-directing agent is the same. In addition, a signal that was related to a five-coordinated Al (20.4 ppm) was observed, suggesting that a portion of the water that existed in the 12-MRs was lost during the freeze-drying process. To determine the water content in the APMeP150, we performed thermogravimetric analysis (TGA); the TG curve is shown in Fig.S4 in the Supporting Information. The result suggests that the APMeP150 in this study lost a mass of approximately 6.3% at 150 °C. In the previous study, a mass loss of 15% at 120°C was observed.<sup>52</sup> Therefore, the TGA analysis is consistent with our speculation that a portion of the water was lost during the freeze-drying process.

When the initial mixture was heated to 200 °C (Fig. 3 (b)), the coordination state of Al underwent a different evolution process.

The intensity of the signal at 44.0 ppm remained nearly constant before long-range ordering was observed (after 30 minutes of heating). Long-range ordering was observed after 50 minutes of heating, and the intensity of this signal decreased slightly and shifted to 43.0 ppm. Subsequently, the intensity of this signal increased and finally shifted to 38.0 ppm after 720 minutes of heating. Contrary to the result after heating to 150 °C (Fig. 3(a)), heating to 200 °C resulted in the signal at -11.3 ppm, which was attributed to the typical octahedral Al that existed during most of the crystallization process and disappeared after 720 minutes of heating. According to the single-crystal structure data, there are nine crystallographically independent four-coordinated Al atoms, which should produce nine resonances in the NMR spectrum. However, only one asymmetric signal that was centred at 38.0 ppm was observed because these crystallographically independent Al sites had similar isotropic chemical shifts. In addition, the broadening effect due to the large anisotropy of the chemical shift and the second-order quadrupolar coupling would lead to the overlap and the inability to distinguish these signals.

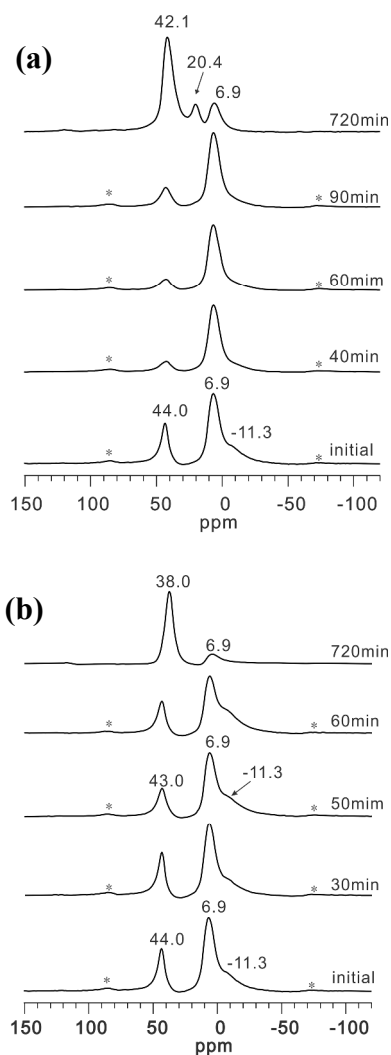


**Fig. 3** The  $^{27}\text{Al}$  MAS NMR spectra of the isolated solid samples that were obtained throughout the hydrothermal treatment period of APMep150 (a) and APMep200 (b). The asterisks indicate spinning side bands.

environment of the P sites; therefore, the crystallization process of the APMep150 and APMep200 was investigated using  $^{31}\text{P}$  MAS NMR spectroscopy. For the APMep150 (Fig. 4(a)), a broad signal at *ca.*-11.3 ppm was observed in the initial mixture, which was assigned to an amorphous aluminophosphate.<sup>25, 54-59</sup> The coordination number of the P atoms to the other non-oxygen atoms varied from 0 to 4, resulting in a broad signal. The signal at -6.3 ppm could be due to the formation of the phosphates in the amorphous phase.<sup>59</sup> Upon heating to 150°C for 40 minutes, the shape of this broad signal slightly changed, and a weak shoulder peak at -18.3 ppm began to appear. After 60 minutes of heating, when the XRD detectable long-range ordering of APMep150 was initially observed, the position of the primary signals did not effectively change, but the intensity of the shoulder peak at -18.3 ppm increased slightly (Fig. 4(a)). The weak shoulder peak at -18.3 ppm was more pronounced after 90 minutes of heating. After 720 minutes of heating, at which time the highly crystalline and pure APMep150 was obtained, an intense signal at -18.3 ppm and a shoulder resonance at -16.8 ppm were observed. The loss of the amorphous phases was shown by the disappearance of the signals at -6.3 and -11.3 ppm. A deconvolution of the spectrum indicated that the ratio of the intensities of these two signals was approximately 3:1. Based on the structural data, the signal at -18.3 ppm can be assigned to P2 and P4, which form the “corner P” of the capped 6-MRs (see Fig. 1(a)), whereas the signal at -16.8 ppm can be assigned to P1 and P3, which form the “cap P” of the capped 6-MRs (see Fig. 1(a)). However, these two signals were located at -21 and -18 ppm, respectively, in the previous study<sup>52</sup> where the authors also analyzed a material with the same topological structure but was synthesized in the presence of 1,4-diaminobutane using an NMR technique, which contains only the tetrahedral Al atoms. Interestingly, the NMR spectrum of the latter compound is composed of an asymmetric line at -18 ppm with a shoulder signal at -17 ppm, and the relative intensities have a ratio of 3:1. Because the structure contains only tetrahedral Al atoms, the shoulder resonance at -17 ppm was unambiguously assigned to the P that was capping the 6-MRs, i.e., the “cap P” of the capped 6-MRs, whereas the signal at -18 ppm was assigned to the P that was within the 6-MR, i.e., the “corner P” of the capped 6-MRs. This result is similar with the result in this study. Thus, we speculated that a portion of the water might be lost during the drying process, which led to the absence of the signal of the six-coordinated Al in the  $^{27}\text{Al}$  MAS NMR spectra (see Fig. 3(a)) and the similarity of the  $^{31}\text{P}$  MAS NMR spectrum of the highly crystalline APMep150 with the  $^{31}\text{P}$  MAS NMR spectrum that was directed by 1,4-diaminobutane. This speculation was supported by the TG analysis results of the highly crystalline APMep150 compound.

The evolution of the coordination state of P in the initial mixture that was heated to 200°C was different from that heated to 150°C. The shape of the spectra of the 30, 50, and 60 minute samples were similar (Fig. 4(b)). After 30 minutes of heating, a shoulder signal at -17.6 ppm was observed, suggesting that the coordination number of P to Al via oxygen atoms increased and that highly polymerized fragments started to form. After heating for 50 and 60 minutes when long-range ordering of the APMep200 compound was observed, the intensity of the shoulder signal at -17.6 ppm increased. After heating for 720

The  $^{31}\text{P}$  NMR spectrum is sensitive to changes in the local

minutes when the highly crystalline APMeP200 compound was formed (see Fig. 2(b)), only a weak resonance that was centered at -11.3 ppm and a strong resonance that was centered at -21.3 ppm were observed. The former resonance signal was from the P with a low coordination number in the initial un-reacted mixture. According to the single-crystal structure data, there are twelve crystallographically independent P atoms in the unit cell, which should have twelve NMR resonances. However, only one dominating signal at -21.3 ppm was observed, suggesting the overlap of the similar chemical shifts of these P sites.

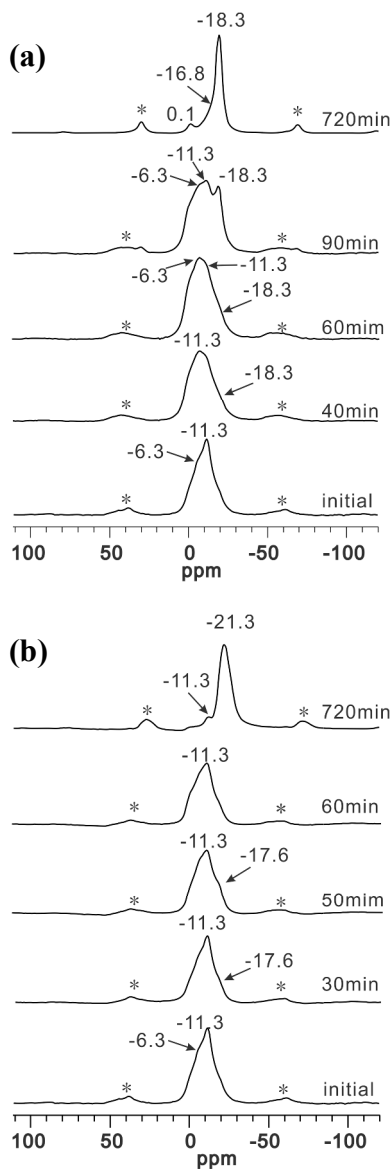


**Fig. 4** The  $^{31}\text{P}$  MAS NMR spectra of the isolated solid samples that were obtained throughout the hydrothermal treatment period of APMeP150 (a) and APMeP200 (b). The asterisks indicate spinning side bands.

The structure of the APMeP200 compound is nearly identical to that of AP2pip, a compound that is synthesized in the presence of piperazine.<sup>53</sup> Using multiple techniques, we have investigated in detail the crystallization process of AP2pip.<sup>33</sup> Interestingly, the crystallization processes of AP2pip and APMeP200 are different, thus, providing an opportunity to investigate the nature of the

structure-directing effect of organic amines and the reason that compounds with the same structures undergo different crystallization processes. This investigation will be completed in the near future and discussed in detail elsewhere.

The APMeP150 and APMeP200 are crystallized from the same initial mixture; the only variable in the crystallization process is the heating temperature. Therefore, the heating temperature affected the structure-directing effect of 2-methylpiperazine and, subsequently, altered the evolution pathway of the initial mixture, i.e. the crystallization process. To elucidate the effect of the heating temperature on the structure-directing effect of 2-methylpiperazine, we investigated the bond lengths of the C-C and C-N bonds in the unique 2-methylpiperazine found in APMeP150 and APMeP200; the data are summarized in Table S5 in the Supporting Information. In the APMeP150, there is only one unique 2-methylpiperazine, whereas there are four and a half unique 2-methylpiperazine in APMeP200. Of the unique 2-methylpiperazine, the fifth half has two possible orientations, resulting in a disorder of this organic amine and an unreasonable bond length of 1.127 Å for the C-C<sub>methyl</sub>. The data in Table S5 show that the heating temperatures of 150 and 200°C changed the structure of 2-methylpiperazine, altering its charge distribution. In both APMeP150 and APMeP200, the 2-methylpiperazine is located in the interlayer region, which indicates that the 2-methylpiperazine might be surrounded by the small building fragments at the beginning of the crystallization. Thus, (1) the strength and direction of the interaction between the 2-methylpiperazine and the small building fragments might be one of the origins of the structure-directing effect, which greatly depends on the structure of the 2-methylpiperazine, (2) the type and structure of the small building fragments formed during the crystallization might also play an important role in determining the final structure, which indicates that the type and structure of the small fragments are part of the structure-directing effect. The fact that the structure of the 2-methylpiperazine in the APMeP150 is significantly different to that in the APMeP200 indicates that the strength and direction of the interaction between the 2-methylpiperazine and the small building fragments at 150°C and 200°C is different from each other. Therefore, the heating temperature affects the structure-directing effect of 2-methylpiperazine via altering its structure. In addition, the different evolution pathways of the concentration of Al and P in the liquids and the pH of the liquid at 150 and 200°C suggested that the change in the heating temperature could significantly alter the equilibrium of the reactions occurring among the source materials and, thus, result in different oligomers or small building fragments, which are also important in determining the final product. Therefore, the heating temperature may affect the structure-directing effect of 2-methylpiperazine via these two ways.

### 3.3 The core units of APMeP150 and APMeP200

Recently, we developed a strategy to investigate the crystallization processes of microporous crystalline compounds by describing the possible building fragments that are formed in the early stages of the crystallization process.<sup>18, 29</sup> The foundation of this strategy is a “reverse temporal evolution” process. With this strategy, the structural information about the small building fragments (species) that are possibly formed during the

crystallization process or the structural information about a “core unit” from which a single crystal might be grown could be obtained. To apply this strategy, we determined the crystallographically unique guest species. Subsequently, the virtual spheres that centre the crystallographically unique guest species (i.e., the N atoms of MeP) were introduced to detect the relative position (close contacts) of the nearby inorganic species in the three-dimensional space. The radius of the sphere can vary from 3.0 to 4.0 Å, or longer. The close contacts between the guest and the inorganic species within the sphere were determined. These close contacts formed a “core unit” with a specific configuration and a hydrogen-bond network (if available) for each open-framework structure. The core unit might be an entity from which a single crystal grew or an entity that was formed during the crystallization process of a single crystal. By applying this strategy, we obtained the core units of the APMep150 and APMep200, with the radius of the virtual sphere of 3.0 Å (the distance to form a strong H-bond), which are shown in Fig. 5(a) and Fig. 5(b), respectively. Even though the water molecules were described in the literature, the exact number and positions of the water molecules are not fully provided in the structure files deposited at the Cambridge Crystallographic Data Centre. Therefore, the water molecules are omitted in the analysis.

Fig. 5(a) shows the core unit of the APMep150 with the radius of the virtual sphere of 3.0 Å. The close contacts between the N atom of 2-methylpiperazine and the O atom of the framework within the 3.0 Å distance are found and labeled. There are strong H-bonds between the structure-directing agent and the inorganic species. There are two unique Al atoms (Al1 and Al2), four unique P atoms (P1, P2, P3, and P4), and one 2-methylpiperazine molecule in the asymmetric unit of APMep150, forming an entity with two P-Al-P trimers and a doubly protonated 2-methylpiperazine. With crystallization, this entity may capture more small building fragments and doubly protonated 2-methylpiperazine molecules via strong H-bonding. With the assistance of other factors, such as indirectly contacted species (aluminato ions, phosphate ions, aluminophosphate ions, and/or doubly protonated 2-methylpiperazine), water molecules, and temperature (for example, heating the same initial mixture at a temperature of 200 °C results in the formation of APMep200, a completely different structure), the P-capped six-membered rings are formed. Upon crystallization, more small fragments are added to the core unit, and the growth of such topology is completed.

The APMep200 contains nine unique Al atoms, twelve P atoms, and four and a half 2-methylpiperazine molecules in its asymmetric unit. Therefore, the core unit of the APMep200 with the radius of the virtual sphere of 3.0 Å is more complicated than that of the APMep150, as shown in Fig. 5(b). This core unit is subtracted from the periodic structure of the APMep200 compound; thus, the core unit, in whole or in part, in the appropriate form, must be formed during crystallization. Therefore, the onset of crystallization of APMep200 must be simpler than the assembly of the core unit shown in Fig. 5(b). A simulation study on the crystallization process of the APMep200 compound might be helpful in understanding the events that occur in the early stage of crystallization.

To clearly understand the events happened in the early stage of the crystallization, it is very necessary to know the exact

structure of the small building fragments. However, due to the limitation of the physical resolution and time resolution of the present characterization techniques, the exact structure of the small building fragments has not been unambiguously determined yet. Among the characterization techniques, electrospray ionization mass spectrometry (ESI-MS) may provide more clues in figuring out the structure of the small building fragments, which has been successfully employed to monitor silicate speciation in pre-nucleating and nucleation zeolitic solutions.<sup>60</sup> Combing the experimentally obtained data of the mass to charge ratio ( $m/z$ ) of the species in the solution, the quantum chemical calculations, and other characterization techniques such as NMR, the structure information of the small building fragments may be indirectly obtained. The application of the ESI-MS on the crystallization process of open-framework aluminophosphate may also provide some useful information about the structure of the small building fragments or core units.

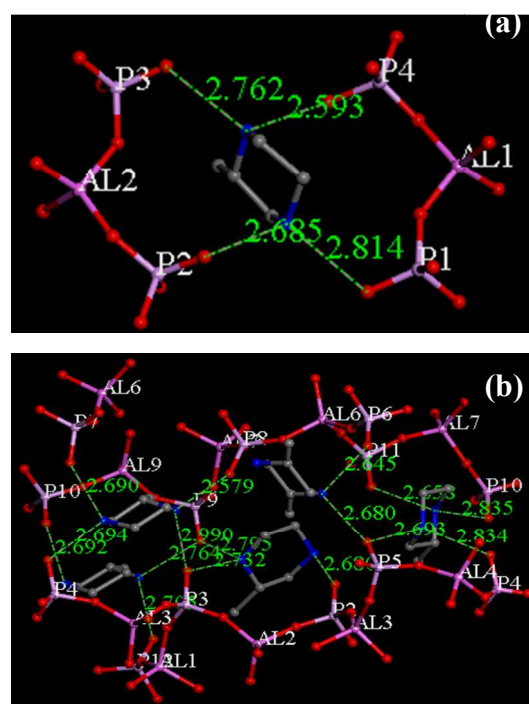


Fig. 5 The core units of the APMep150 (a) and APMep200 (b) with the radius of the virtual sphere of 3.0 Å.

### 3.4 Stability of the core unit of APMep150

Because the APMep150 and APMep200 were crystallized from the same initial mixture and the only difference in the synthetic conditions is the heating temperature, it would be interesting to know if the core unit of APMep150 is less stable than that of APMep200 and if APMep150 will be finally changed to APMep200 with prolonged heating time. In the X-ray diffraction investigation of the crystallization process of APMep150, it can be observed that the long-range ordering of APMep150 just starts appearing when the heating time reached 60 minutes. Thus, a large number of core units of APMep150 should be formed at this time. Experimentally, the same amount of initial mixture was loaded into two autoclaves and heated at 150°C. When the heating time reached 60 minutes, one autoclave was quenched with cold water and the solid sample was characterized with X-

ray diffraction. The other autoclave was quickly moved to the 200°C oven. When the heating time reached 720 minutes, the autoclave was quenched with cold water the solid sample was characterized with X-ray diffraction. Fig. 6 shows the simulated XRD pattern of APMep150 and the experimental patterns of both solid samples. The results in Fig. 6 suggest that the core units of APMep150 are stable and can further grow to crystals of APMep150 at 200°C; the formation of the core units of APMep200 is not observed even though the heating temperature is 200°C. When the initial mixture is heated at 150°C for 60 minutes, it is expected that a large number of core units of APMep150 are formed. Thus, the composition of the other part of the mixture should be different to that of the initial mixture that favours the formation of the core unit of APMep200 at 200°C. When the autoclave is further heated at 200°C, the core unit of APMep200 cannot be formed.

To investigate if the APMep150 is an intermediate of APMep200, we prolonged the heating time at 150°C to 1, 3, 7, and 15 days, which is about 30 times longer than the time needed for the full crystallization of APMep150. The XRD patterns of these products are provided in Fig.S5 in the Supporting Information. Clearly, no XRD-detectable APMep200 is observed. These results suggest that APMep150 is not an intermediate of APMep200.

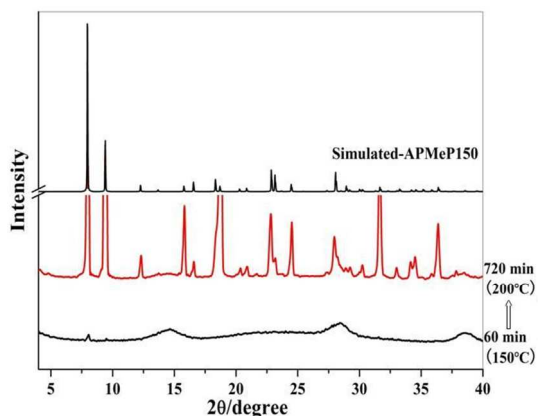


Fig.6 The simulated XRD pattern of APMep150 and the experimental XRD patterns of the solid samples heated at 150 °C for 60 minutes and first heated at 150°C for 60 minutes then at 200°C for 720 minutes.

#### 4. Conclusions

In summary, the layered aluminophosphates, APMep150 and APMep200, are synthesized from the same initial mixture with the composition of  $\text{Al}_2\text{O}_3\cdot\text{P}_2\text{O}_5\cdot 1.5\text{MeP}\cdot 125\text{H}_2\text{O}$  at 150 and 200°C, respectively. The crystallization processes of both compounds are thoroughly characterized using XRD, pH, elemental, and NMR analyses. The evolution of the coordination state of Al and P in the initial mixture at the heating temperature of 150°C is significantly different with that at the heating temperature of 200°C, suggesting that the oligomers or building fragments of the aluminophosphate that were formed during the two syntheses are different from each other. The control experiments show that the core units of APMep150 are stable at 200°C and the formation of a specific core unit needs the right gel composition. At 150°C, the APMep150 is not an intermediate of APMep200. The chemical properties of the structure-directing

agent 2-methylpiperazine at the heating temperature of 150°C is also significantly different with that at the heating temperature of 200°C, indicating that the interactions between 2-methylpiperazine and the oligomers or building fragments of the aluminophosphate during the two syntheses are different from each other. The application of the “reverse temporal evolution” process to both structures results in two different core units or possible onsets of crystallization. The heating temperature can affect crystallization process of the initial mixture and the structure-directing effect of 2-methylpiperazine by altering its structure, changing the equilibrium of the reactions occurring among the source materials, and modifying the assembly of the building oligomers.

#### Acknowledgment

We acknowledge the special funding support from the National Natural Science Foundation of China (21171063), the Excellent Young Scientists Fund (21222103), the State Basic Research Projects of China (2011CB808703), and the Specialized Research Fund for the Doctoral Program of Higher Education

#### Notes and references

- <sup>a</sup> State Key Laboratory of Inorganic Synthesis and Preparative Chemistry, College of Chemistry, Jilin University, 2699 Qianjin Street, Changchun 130012, PR China. Fax: +86-431-85168609; Tel: +86-431-85168609; E-mail: [yanw@jlu.edu.cn](mailto:yanw@jlu.edu.cn)
  - <sup>b</sup> Wuhan Center for Magnetic Resonance, State Key Laboratory of Magnetic Resonance and Atomic and Molecular Physics, Wuhan Institute of Physics and Mathematics, The Chinese Academy of Sciences, Wuhan 430071, PR China.
- †Electronic Supplementary Information (ESI) available: The plots and values of the concentrations of Al and P and the pH of the liquid phases, the TG curve of APMep150, The XRD patterns of APMep150 at 150°C for 1, 3, 7, and 15 days, The bond lengths of the C-C and C-N bonds in the unique MeP molecules in APMep150 and APMep200. See DOI: 10.1039/b000000x/
- ‡ These authors contributed equally to this work.
- R. Xu, W. Pang, J. Yu, Q. Huo and J. Chen, *Chemistry of Zeolites and Related Porous Materials: Synthesis and Structure*, John Wiley & Sons (Asia) Pte Ltd, Singapore, 2007.
  - J. Cejka, A. Corma and S. I. Zones, eds., *Zeolites and Catalysis-Synthesis, Reactions and Applications*, WILEY-VCH Verlag GmbH & Co. KGaA, Weinheim, 2010.
  - S. Kulprathipanja, ed., *Zeolites in Industrial Separation and Catalysis*, WILEY-VCH Verlag GmbH & Co. KGaA, Weinheim, 2010.
  - C. S. Cundy and P. A. Cox, *Micropor. Mesopor. Mater.*, 2005, 82, 1-78.
  - D. W. Breck, *Zeolite Molecular Sieves*, Wiley, New York, 1974.
  - S. T. Wilson, B. M. Lok and E. M. Flanigen, *U.S. Patent*, 4,310,440, 1982.
  - S. T. Wilson, B. M. Lok, C. A. Messina, T. R. Cannan and E. M. Flanigen, *J. Am. Chem. Soc.*, 1982, 104, 1146-1147.
  - J. H. Yu and R. R. Xu, *Acc. Chem. Res.*, 2003, 36, 481-490.
  - J. H. Yu and R. R. Xu, *Chem. Soc. Rev.*, 2006, 35, 593-604.
  - W. F. Yan, J. H. Yu, R. R. Xu, G. S. Zhu, F. S. Xiao, Y. Han, K. Sugiyama and O. Terasaki, *Chem. Mater.*, 2000, 12, 2517-2519.
  - C. Baerlocher and L. B. McCusker, Database of Zeolite Structures, <http://www.iza-structure.org/databases/>.
  - S. T. Wilson, B. M. Lok, C. A. Messina, T. R. Cannan and E. M. Flanigen, in *Intrazeolite Chemistry*, eds. G. D. Stucky and F. G. Dwyer, Am. Chem. Soc., Washington, D. C., 1983, vol. 218, ch. 5, pp. 79-106.
  - N. J. Tapp, N. B. Milestone and D. M. Bibby, *Zeolites*, 1988, 8, 183-188.
  - S. Kumar, Z. P. Wang, R. L. Penn and M. Tsapatsis, *J. Am. Chem. Soc.*, 2008, 130, 17284-17286.

15. F. T. Fan, Z. C. Feng, K. J. Sun, M. L. Guo, Q. Guo, Y. Song, W. X. Li and C. Li, *Angew. Chem.-Int. Ed.*, 2009, 48, 8743-8747.
16. C. Kosanovic, K. Havancsak, B. Subotic, V. Svetlicic, T. Mistic, A. Cziraki and G. Huhn, *Micropor. Mesopor. Mater.*, 2009, 123, 150-159.
17. B. Tokay, M. Somer, A. Erdem-Senatalar, F. Schuth and R. W. Thompson, *Micropor. Mesopor. Mater.*, 2009, 118, 143-151.
18. W. F. Yan, X. W. Song and R. R. Xu, *Micropor. Mesopor. Mater.*, 2009, 123, 50-62.
19. A. Aerts, C. E. A. Kirschhock and J. A. Martens, *Chem. Soc. Rev.*, 2010, 39, 4626-4642.
20. F. T. Fan, Z. C. Feng and C. Li, *Chem. Soc. Rev.*, 2010, 39, 4794-4801.
21. W. F. Yan, L. Xin, V. Olman, J. H. Yu, Y. Wang, Y. Xu and R. R. Xu, *Micropor. Mesopor. Mater.*, 2010, 131, 148-161.
22. A. Aerts, L. R. A. Follens, E. Biermans, S. Bals, G. Van Tendeloo, B. Loppinet, C. E. A. Kirschhock and J. A. Martens, *Phys. Chem. Chem. Phys.*, 2011, 13, 4318-4325.
23. A. Depla, E. Verheyen, A. Veyfeyken, E. Gobechiya, T. Hartmann, R. Schaefer, J. A. Martens and C. E. A. Kirschhock, *Phys. Chem. Chem. Phys.*, 2011, 13, 13730-13737.
24. C. Kosanovic, K. Havancsak, B. Subotic, V. Svetlicic, T. M. Radic, A. Cziraki, G. Huhn, I. Buljan and V. Smrecki, *Micropor. Mesopor. Mater.*, 2011, 142, 139-146.
25. B. Zhang, J. Xu, F. T. Fan, Q. Guo, X. Tong, W. F. Yan, J. H. Yu, F. Deng, C. Li and R. R. Xu, *Micropor. Mesopor. Mater.*, 2012, 147, 212-221.
26. S. Kumar, R. L. Penn and M. Tsapatsis, *Micropor. Mesopor. Mater.*, 2011, 144, 74-81.
27. A. Palcic, J. Bronic, D. Brlek and B. Subotic, *Crystengcomm*, 2011, 13, 1215-1220.
28. L. M. Ren, C. J. Li, F. T. Fan, Q. Guo, D. S. Liang, Z. C. Feng, C. Li, S. G. Li and F. S. Xiao, *Chem.-Eur. J.*, 2011, 17, 6162-6169.
29. T. Cheng, J. Xu, X. Li, Y. Li, B. Zhang, W. F. Yan, J. H. Yu, H. Sun, F. Deng and R. R. Xu, *Micropor. Mesopor. Mater.*, 2012, 152, 190-207.
30. N. Hould, M. Haouas, V. Nikolakis, F. Taulelle and R. Lobo, *Chem. Mater.*, 2012, 24, 3621-3632.
31. R. Garcia, L. Gomez-Hortiguera, F. Sanchez and J. Perez-Pariente, *Micropor. Mesopor. Mater.*, 2011, 146, 57-68.
32. A. Samadi-Maybodi, S. K. H. Nejad-Darzi and M. Tafazzoli, *J. Solut. Chem.*, 2012, 41, 888-897.
33. X. Q. Tong, J. Xu, C. Wang, H. Y. Lu, P. Huang, W. F. Yan, J. H. Yu, F. Deng and R. R. Xu, *Micropor. Mesopor. Mater.*, 2012, 155, 153-166.
34. S. Araki, Y. Kiyohara, S. Tanaka and Y. Miyake, *J. Colloid Interface Sci.*, 2012, 376, 28-33.
35. N. Ren, B. Subotic, J. Bronic, Y. Tang, M. D. Sikiric, T. Mistic, V. Svetlicic, S. Bosnar and T. A. Jelic, *Chem. Mater.*, 2012, 24, 1726-1737.
36. E. A. Eilertsen, M. Haouas, A. B. Pinar, N. D. Hould, R. F. Lobo, K. P. Lillerud and F. Taulelle, *Chem. Mater.*, 2012, 24, 571-578.
37. A. Rojas, L. Gomez-Hortiguera and M. A. Cambor, *J. Am. Chem. Soc.*, 2012, 134, 3845-3856.
38. Z. C. Zhao, W. P. Zhang, R. S. Xu, X. W. Han, Z. J. Tian and X. H. Bao, *Dalton Trans.*, 2012, 41, 990-994.
39. X. Q. Tong, J. Xu, L. Xin, P. Huang, H. Y. Lu, C. Wang, W. F. Yan, J. H. Yu, F. Deng, H. Sun and R. R. Xu, *Micropor. Mesopor. Mater.*, 2012, 164, 56-66.
40. C. E. White and J. L. Provis, *J. Phys. Chem. C*, 2012, 116, 1619-1621.
41. X. Q. Zhang, T. T. Trinh, R. A. van Santen and A. P. J. Jansen, *J. Phys. Chem. C*, 2011, 115, 9561-9567.
42. X. Q. Zhang, T. T. Trinh, R. A. van Santen and A. P. J. Jansen, *J. Phys. Chem. C*, 2012, 116, 1622-1623.
43. X. Tong, J. Xu, X. Li, Y. Li, W. Yan, J. Yu, F. Deng, H. Sun and R. Xu, *Micropor. Mesopor. Mater.*, 2013, 176, 112-122.
44. R. M. Shayib, N. C. George, R. Seshadri, A. W. Burton, S. I. Zones and B. F. Chmelka, *J. Am. Chem. Soc.*, 2011, 133, 18728-18741.
45. L. Zhang, J. Bates, D. H. Chen, H. Y. Nie and Y. N. Huang, *J. Phys. Chem. C*, 2011, 115, 22309-22319.
46. A. M. Beale, M. G. O'Brien, M. Kasunic, A. Golobic, M. Sanchez-Sanchez, A. J. W. Lobo, D. W. Lewis, D. S. Wragg, S. Nikitenko, W. Bras and B. M. Weckhuysen, *J. Phys. Chem. C*, 2011, 115, 6331-6340.
47. B. H. Chen and Y. N. Huang, *Micropor. Mesopor. Mater.*, 2011, 143, 14-21.
48. X. Q. Zhang, T. T. Trinh, R. A. van Santen and A. P. J. Jansen, *J. Am. Chem. Soc.*, 2011, 133, 6613-6625.
49. X. Tong, J. Xu, C. Wang, W. Yan, J. Yu, F. Deng and R. Xu, *Micropor. Mesopor. Mater.*, 2014, 183, 108-116.
50. H. Lu, Y. Yan, X. Tong, W. Yan, J. Yu and R. Xu, *Sci China Chem*, 2014, 57, 127-134.
51. X. Tong, H. Lu, P. Huang, W. Yan, J. Yu and R. Xu, *Chinese J. Inorg. Chem.*, 2013, 29, 1639-1644.
52. A. Tuel, V. Gramlich and C. Baerlocher, *Micropor. Mesopor. Mater.*, 2002, 56, 119-130.
53. A. Tuel, V. Gramlich and C. Baerlocher, *Micropor. Mesopor. Mater.*, 2001, 46, 57-66.
54. A. R. Grimmer and U. Haubenreisser, *Chem. Phys. Lett.*, 1983, 99, 487-490.
55. I. L. Mudrakovskii, V. P. Shmachkova, N. S. Kotsarenko and V. M. Mastikhin, *J. Phys. Chem. Solids*, 1986, 47, 335-339.
56. P. Hartmann, J. Vogel and B. Schnabel, *J. Magn. Reson. Ser. A*, 1994, 111, 110-114.
57. J. Xu, L. Chen, D. L. Zeng, J. Yang, M. J. Zhang, C. H. Ye and F. Deng, *J. Phys. Chem. B*, 2007, 111, 7105-7113.
58. C. P. Grey and A. J. Vega, *J. Am. Chem. Soc.*, 1995, 117, 8232-8242.
59. J. Xu, D. Zhou, X. W. Song, L. Chen, J. H. Yu, C. H. Ye and F. Deng, *Micropor. Mesopor. Mater.*, 2008, 115, 576-584.
60. I. H. Lim, W. Schrader and F. Schuth, *Micropor. Mesopor. Mater.*, 2013, 166, 20-36.